Ocular Electromyographic Control of Servos

Milo J. Hooper

6.101 Spring 2019

Abstract

This project seeks to control servo motors to determine the position of a target laser based on the motions of eye muscles. The electromyographic signals generated by muscle contraction and relaxation near the human eye will be collected via electrodes placed adjacent to the eye. The basic objective is to be able to determine when and in what orientation eyes move, requiring significant signal processing. As an intermediate goal, I will mount PWM-controlled continuous rotation servos onto each other and use the signals from the EMG to direct a laser beam that can be viewed on a wall. If time permitted, I would have attempted to insert a fiber-optic layer in the apparatus allowing electrically wireless control.

Contents

Chapter 1

Introduction

1.1 Motivation

Inspiration for this project arose from a desire to integrate newfound electronics knowledge with the human body. Another class I took this semester, 2.184 (Biomechanics and Neural Control of Movement) covered content relating to electromyographic signals. I had never heard of this phenomenon before and became interested in investigating it for my 6.101 project.

Processing electromyographic signals has significant potential benefits in the development of prosthetic and assistive technologies, allowing for human control of a variety of mechanisms and elements actuated remotely by signals normally intended for muscles.

1.2 Objectives

The set of goals for this project began with basic functionality and added increasingly interesting elements to the circuit.

Minimum Goals: Detecting the Signal

- Unique signals are visible on an oscilloscope generated upon eye movements: Left, Right, Up, Down, Blink
- 4th order filter functions as designed: attenuates 60Hz noise and amplifies differential signal output from instrumentation amplifier 2000x
- Activates different switches/indicators (LEDs) depending on eye movement input

Basic Goals: Utilizing the Signal

- Astable oscillator functions to generate 1ms, 1.5ms, and 2ms 50Hz PWM signals that can be input to the servo motor
- The motors spin on these inputs
- The inputs are accurately determined by eye movements (replacing LED setup with FET gates to control resistor values in the astable oscillator)

Stretch Goals: Extending Utilization of the Signal

- Adding another energy domain: light / fiber optic control of the servos
- Multiplexes the signals for left/right and up/down into one channel transmitted into the fiber optic cable
- Demultiplexes and determines intended movements for the motors
- The motors function as in Basic Goals, but now removed from the eye motion gates by the fiber-optic stage.

Chapter 2

Design Approach

2.1 Block Diagram

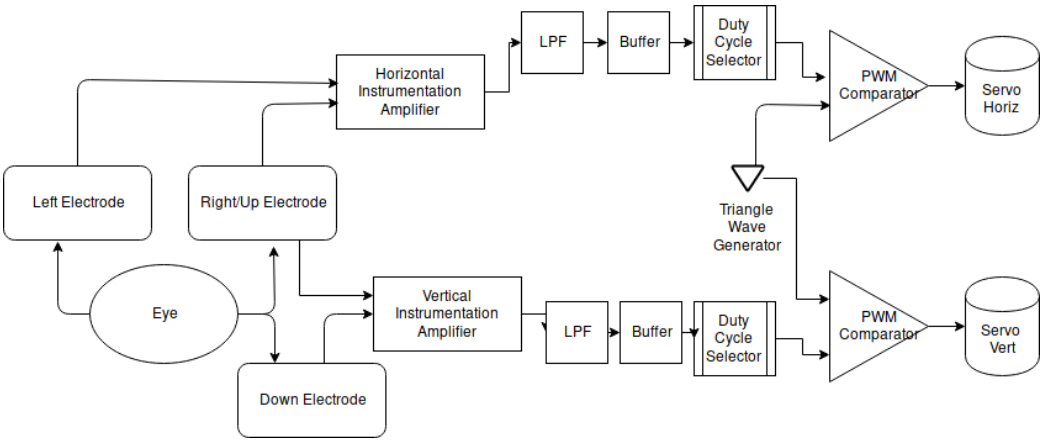

Figure 2.1: High-Level System Block Diagram

2.2 Functional Stages

2.2.1 General Notes

The system for processing the EMG signal is as shown in the above block diagram. Signals are fed into instrumentation differential amplifiers, sent

through low-pass filters, and amplified such that combinations of them can be matched to different DC voltages that can be compared against a 555-generated triangle wave that creates servo PWM signals. Thus servo motors are driven by eye movements.

All operational amplifiers, unless otherwise specified, were LF356 JFET Input Operational Amplifiers. This is due to their flexible range of use cases and general availability in lab.

All resistors were used with 5% tolerances.

When feasible, all RC networks utilized 470nF capacitors (10% tolerance) due to their being the largest non-electrolytic capacitors available.

2.2.2 Signal Acquisition

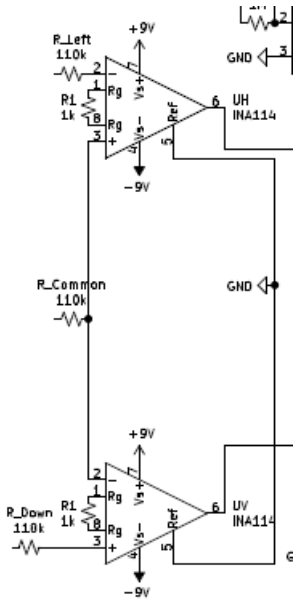

Figure 2.2: Instrumentation Amplifiers

The most difficult part of this project was largely getting a consistent readout of the electromyographic signals from the eye. Unaided by amplification, the EMG signals show up on an oscilloscope as nearly imperceptible 0.5-2mV bumps on 100mV 60Hz sinusoidal waveforms.

EMG signals are not easily observed when one electrode is compared with a constant reference ground. The phenomenon is discovered when one

observes the differential signal between two electrodes.

A triangular arrangement of electrodes placed around the right eye allowed for a minimization of the number of electrodes needed to accomplish two-axis signal detection by utilizing the upper-right electrode as a common signal potential for processing in both channels.

For the purpose of personal safety, $110k\Omega$ resistors were put in direct connection between any electrodes and the rest of the circuit.

To reduce the influence of common mode noise and amplify gain , the INA114 Precision Instrumentation Amplifier was used for each channel. This allowed for high common-mode attenuation while significantly amplifying the differential signal.

Differential gain in the INA114 is controlled via a single resistor placed from pins 1 to 8, following the relation:

$$G = 1 + \frac{50k\Omega}{R_G}$$

Initially, a 100Ω value was used for R_G to produce a gain of approximately 500 to be passed into the following stage, which at the time was an op-amp buffer feeding into the low-pass filter.

Upon discovering the difficulty that such high gain presented when DC offsets entered into the differential signal, the gain was lowered at this stage to only 50 using $1k\Omega$ resistors, and the signal was passed into a DC Offset topology before filtering. The DC offsets of the two input signals would be amplified, and the output of the instrumentation amplifier would rail, losing the information about the signal that had been riding on top of the 60 Hz waves.

2.2.3 DC Offset Compensation

As considered in the ECG lab for this class, a DC offset adjustment was going to be required for successful and reliable processing of the similar EMG signal.

The offset was achieved independently for each channel by feeding the output of the INA114 into an integrative operational amplifier comparing the output signal from the end of the filter with flat ground, then adding the negative of that offset value via an op-amp adder topology to the original signal before feeding it into the filter stage.

The circuit was originally designed with this element absent, which led to reliability issues in INA114 output.

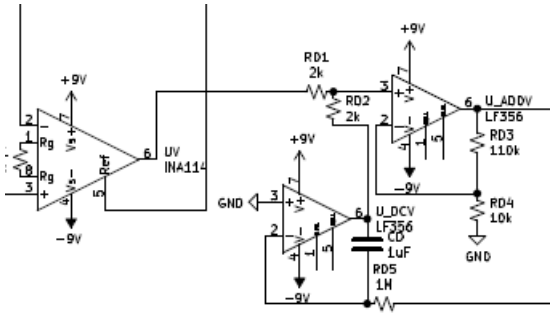

Figure 2.3: DC Offset Compensation

2.2.4 Fourth Order Chebyshev Type I Low-Pass Filter

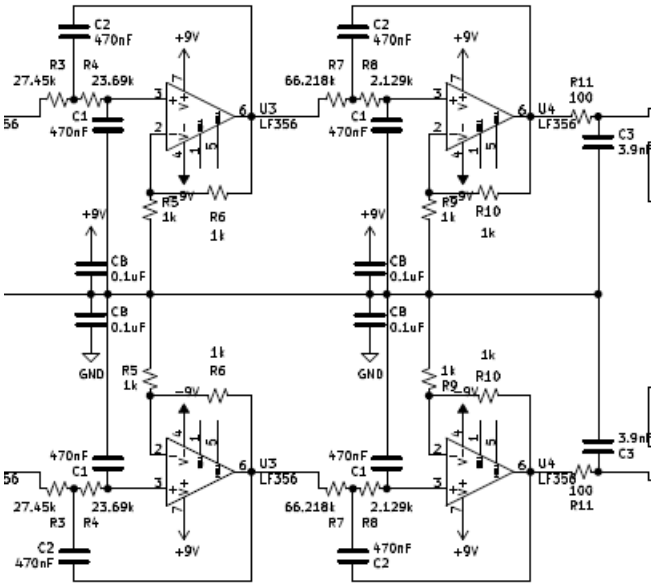

Figure 2.4: 4th-Order Low-Pass Filter

Despite common-mode attenuation and differential signal amplification from the prior stages, there remained significant levels of 60 Hz noise that made reliable analog handling of the EMG signal difficult. To address this, a high order filter was used. A 4th-order filter provided the best balance of high attenuation and spatial compactness as it could be fit around a single

dual op-amp chip, such as the LF353. To achieve a frequency attenuation rolloff stronger than the expected -80 dB/decade associated with a generic 4th-order filter, a filter of the Chebyshev Type I variety was chosen. For simplicity in calculations, physical construction was achieved with cascaded Sallen-Key topologies.

Though the frequency range of EMG signals is from 1-300 Hz in human beings, reading only sub-30 Hz frequencies is sufficient to determine the directional activity of the eye. Thus low-pass filters were chosen. If this were not the case, a sharp notch filter would have been in order.

The frequency response of a Chebyshev Type I filter is unique in that it produces a steep dropoff after the determined cutoff frequency, at the cost of distortive ripple in the passband. (A Type II is the same, but has the distortive ripple in the stopband instead of the passband, and is less useful for this application).

Calculations to determine the locations of the poles of the overarching filter largely followed the suggested method from Texas Instruments [3] in high-order active filter designs:

Define FSF as a frequency scaling factor. Define f_c as a cutoff frequency. Define f as a frequency being considered in evaluation of gain and phase in the transfer function. Define Re and Im as the respective real and imaginary portions of pole locations.

$$FSF = \sqrt{Re^2 + |Im^2|}$$

$$Q = \frac{FSF}{2 * Re}$$

The transfer function of a generic 2nd order filter is as follows:

$$\frac{-K}{(\frac{f}{FSF*f_c})^2 + \frac{1}{Q} * \frac{j*f}{FSF*f_c} + 1}$$

The desired cutoff frequency was chosen as 30Hz. Since some ripple in the passband is acceptable (presence is more important than exact amplitudes here for signal detection), a 3dB ripple can be tolerated. Consulting charts for filter pole placement and locating the entry for 4th-order low-pass Chebyshev Type I produced the following required values: Stage I with $FSF = 0.4426$ and $Q = 1.0765$, and Stage II with $FSF = 0.9503$ and $Q = 5.577$. These values were combined with the 470nF capacitor standard used in the project, as

well as with the fact that the resistors were determined to be scalar multiples of each other for simplicity of calculations.

To further ease calculation, a filter gain K of 2 was decided upon, as this allowed the feedback resistors to be made equivalent (with $1k\Omega$ value). Since there were two stages, the overall filter gain was 4, leading to an overall differential signal gain of 2000. When the system worked, there were easily 1V amplitudes of waves being generated with only approximately 20 mV of 60 Hz ripple – much easier to process than the noisy prefilter waveform.

Assuming that resistor $R_3 = m * R_4$ in a one of these filters, the relations integrating the given values produces a system of three equations in three unknowns:

$$Q = \sqrt{m},$$

$$f_c * FSF = \frac{1}{2 * \pi * R_4 * C * \sqrt{m}},$$

and the above given relation between R_3 and R_4.

These produce values of $R_3 = 27.4k\Omega, R_4 = 23.69k\Omega$ for the first filter stage, and $R_8 = 2.129k\Omega, R_7 = 66.218k\Omega$ for the second stage. As such precise resistor values would be both cost-prohibitive and unnecessary, the nearest 5% tolerance resistors sufficed, with respective nominal values of 27, 24, 2, and 68 $k\Omega$. The rationale for allowing such wide swings in tolerance is that the frequency of interest in attenuation is 60 Hz, and the cutoff in the filter is placed well below that, ideally at 30 Hz. If the actual values place the cutoff at 27 or 33 Hz, the performance will be effectively equivalent, especially due to the Chebyshev filter's steep slope after the cutoff frequency.

To improve high-frequency (on the order of kHz) attenuation a final addition of a 40 kHz passive low-pass filter was used with a resistor of 100Ω in series and a capacitor of 3.9 nF attached subsequently to ground.

2.2.5 Buffering

In order to retain a stable signal at various stages of the system, op-amps in a gainless negative-feedback buffer configuration were utilized heavily.

Buffering occurred critically at the output of the Chebyshev filter, the output of the signal comparators, and the servo PWM generator.

There was initially buffering occurring between the INA114 stage and the Chebyshev filter stage, but that location on the prototyping board was replaced with an LF353 JFET Dual Op-Amp package in order to handle

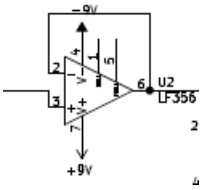

Figure 2.5: One of five identical buffers in the project

DC Offset calibration and addition of the offset to the original signal while requiring the minimum amount of rewiring.

The high input impedance of the LF356 op-amps used in the filter stage made the initial buffers unnecessary, thus the circuit was not adversely affected in functionality by their removal.

2.2.6 Signal Combination Resolution

At this stage of the project, when the prior stages all functioned properly, one could easily detect the waveform combinations that resulted from a variety of eye movements. The combinations are as follows:

Channel	Blink	Up	Right	Left	Down	No Activity
Vertical	HI <0.2s	HI >0.2s	HI	HI	LO	0
Horizontal	0	0	HI	LO	HI	0

Where HIGH signifies a 300mV-1V bump, LOW signifies the negative of that, and 0 signifies a flat waveform.

A series of Schmitt Trigger topologies with op-amps functioning as comparators with various thresholds compared against the integrated average of the waveform digitize the signals into true HIGH and LOW values, with two triggers per channel due to the need to detect three possible states per channel (HIGH, LOW, and 0).

Due to time constraints and difficulty separating "blink" and "up" activity readouts, the detection of blinking was dropped from the possible states being evaluated.

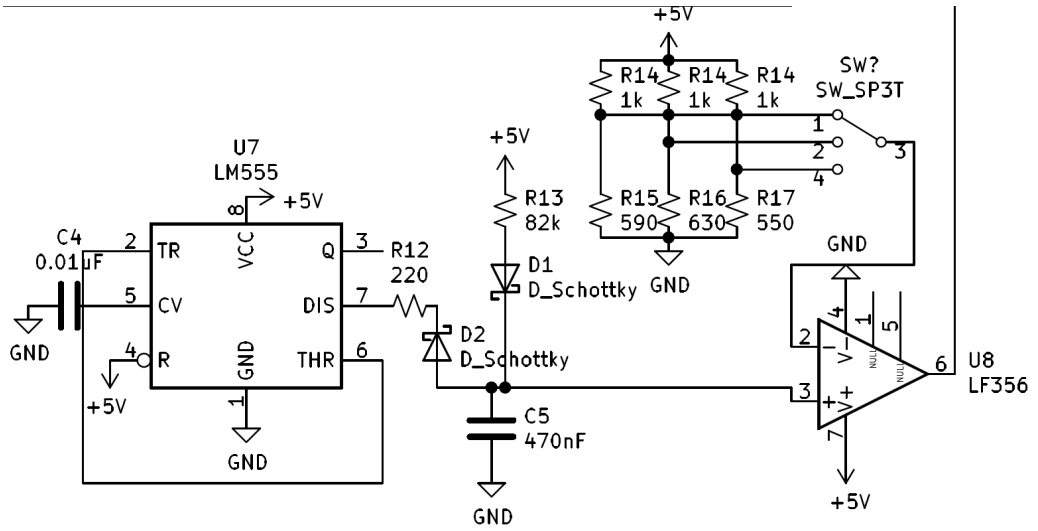

Figure 2.6: Comparing the triangle wave with one of the three DC offsets (represented for simplicity by a single pole triple throw switch). The output of U8 feeds into the signal input of the servo motors.

2.2.7 Servo Control

This project used the SpringRC SM-S4303R continuous rotation servo motors. They are small, lightweight servos that operate between 4.8 and 6 Volts. Direction of servo rotation is determined by the width of the pulses of a PWM signal that operates at approximately 50Hz.

In order to guarantee a stable voltage level for the servos, a 7805 linear regulator supplied 5V to all servo control logic and power supply for relevant op-amps and timers. The 555 Timer chip was used in astable oscillation mode with diode-directed discharge and charge paths to the capacitor for a more usable sawtooth wave output. Schottky diodes were used for their lower forward voltage drop and availability in lab.

The sawtooth was then compared against a DC value generated by a resistive divider from 5V to 0V that is equivalent to 10%, 15%, or 20% of the maximum amplitude of the sawtooth wave. The resulting waveform from the comparator resembled a PWM of duty cycle equivalent to the percentage of maximum voltage produced at the divider.

DC values generated by the resistive dividers would be selected depending on the desired motion of the motors via a series of CMOS gate configurations

that would activate upon aforementioned channel signal high, low, or zero signals, with all-zero signal outputs causing the stall configuration (1.5ms width) to be output to the servos.

To clean up the output of the PWM generator, it was then fed into another comparator stage that would rail the output into a semantically equivalent square wave more suitable for directing into a servo pin.

The output of the triangle wave generator was fixed largely between 3.3 V and 1.6 V. In order to create duty cycles of 10%, 15%, and 20% from this, resistive dividers from $1k\Omega$ down to 590Ω , 630Ω, and 550Ω were used for stall, forward, and backward drives respectively.

2.3 Full Circuit Schematic

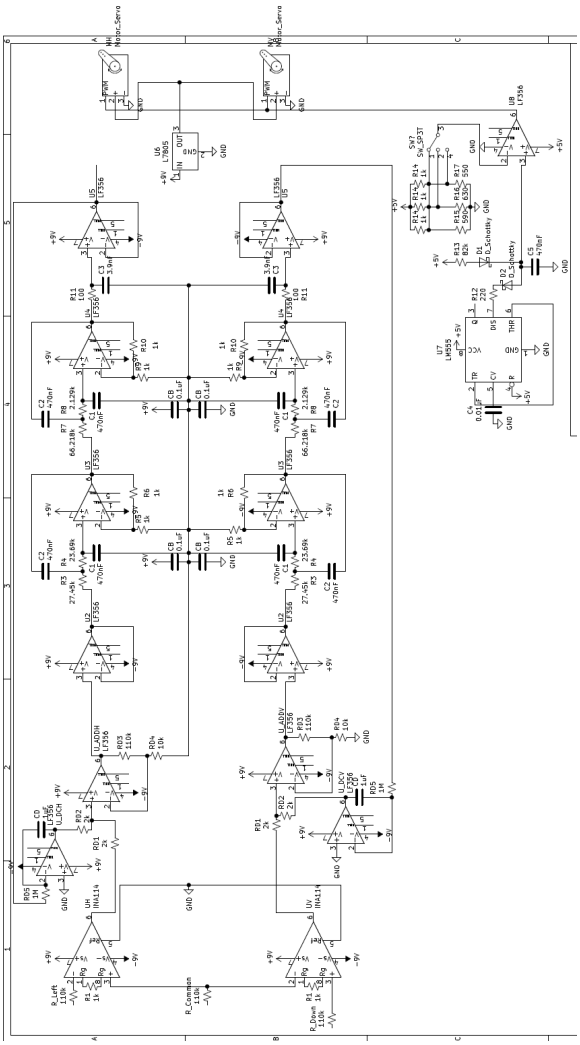

Figure 2.7: Main Schematic

Chapter 3

Challenges

A multitude of difficulties arose in the process of attempting to complete this project's various stages.

3.1 Signal Pickup

One of the most persistent issues was intermittent unreliability of instrumentation amplifier output. The leads from the electrodes were long, and would pick up disturbances such as a person walking behind the test apparatus as readily as the intended signals from eye motion-generated potentials.

Issues that arose from the instrumentation amplifiers were flat DC output or railing 60 Hz noise. These occurred at irregular intervals regardless of the gain resistor. One minute the oscilloscope would show proper functioning of the circuit from the instrumentation amp through the filter stages into the comparators, the next it would rail 60 Hz despite no physical interaction with the circuit occurring.

3.2 Power Supply

Another unexpected challenge that presented itself was sorting out power supply issues. The batteries used in lab, 9 V Ni-MH Power 600 models, had a high internal resistance (approximately 50Ω) and could not supply a stable voltage; while the circuit was in operation, even with batteries connected directly to the power rails, a multimeter would show significant drops in

battery voltage over a short period of time (hundredths of volts over tens of seconds).

Using a dual supply of two 9 volt batteries allowed for a wider voltage swing when attempting to accommodate high-amplitude 60 Hz noise waves, but ultimately did not significantly help the performance of the circuit. The main benefit of the dual supply was the fact that it would remove the need for a buffer after a resistive-divider-generated virtual ground at 4.5 V.

The other difficulty with the batteries arose when attempting to drive servo motors off of the circuit rails. The high current draw from the battery required to power even one servo led to significant voltage drops as a consequence of high internal resistance. Thus the servos drove very slowly, if at all. Powering the servos externally (but referencing all voltages to rail ground) allowed them to spin more easily.

3.3 Compactness versus Ease of Debugging

The original design for this project had compactness as a crucial element. Rather than two separated channels of LF356 op-amp-driven signal processing, all processing took place on half of the physical space using LF353 dual op-amps, which were of the same physical size as the LF356 but had twice as much functionality. Both each channel of processing, rather than operating on an entire breadboard row, operated on only one side of the row.

This approach was functional at times, but suboptimal in that the smallest perturbation or incorrect behavior was incredibly difficult to debug, as all of the capacitors and resistors were pressed into a compact space, making it difficult to swap components or to insert probe leads without accidentally loosening some component.

Another attempt to rectify this situation led to soldering the components onto perfboard and tested stage by stage. Nevertheless, issues persisted in that the instrumentation amplifier would still rail or provide non-useful output. Rather than attempt to resolder and repair that board, the physically separated channels approach was chosen, which allowed for easier isolation of problems in the circuit implementation.

Chapter 4

Conclusion

One way to improve this design would be to implement DC offsetting from the start or replace it entirely with a band-pass filter rather than a low-pass filter. Another is that the placement of electrodes could have been arranged in a set of four rather than three, allowing for fully independent axis-channel processing.

Ultimately, the project was intermittently functional. Signal filtering from the noisy input was achieved, and clear, easily-processed waveform changes occurred at each of the activities that were intended to be detected, namely blinking in addition to eye motion in the horizontal and vertical axes. The servos were able to be successfully driven by the divider-created offsets compared to 50 Hz 555-generated triangle waves and re-compared to more strongly digitize the output. Comparators placed at the end of the filter-buffer stage demonstrated the ability to create square waves with changes in state corresponding closely to changes in activity.

Bibliography

[1] Burr-Brown. Ina114 datasheet. Texas Instruments, 3 1998. http://www.ti.com/lit/ds/symlink/ina114.pdf.

[2] Texas Instruments. Lfx5x datasheet. Texas Instruments, 11 2015. http://www.ti.com/lit/ds/symlink/lf356.pdf.

[3] Jim Karki. Active low-pass filter design. Texas Instruments, 2002. http://www.ti.com/lit/an/sloa049b/sloa049b.pdf.

[4] ServoDatabase.com. Springrc sm-s4303r continuous rotation robot servo datasheet. Web, 2019. https://servodatabase.com/servo/springrc/sm-s4303r.